

# Soft Matter

Accepted Manuscript



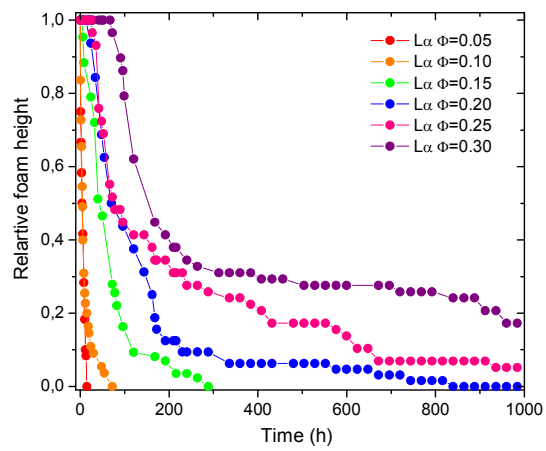
This is an *Accepted Manuscript*, which has been through the Royal Society of Chemistry peer review process and has been accepted for publication.

*Accepted Manuscripts* are published online shortly after acceptance, before technical editing, formatting and proof reading. Using this free service, authors can make their results available to the community, in citable form, before we publish the edited article. We will replace this *Accepted Manuscript* with the edited and formatted *Advance Article* as soon as it is available.

You can find more information about *Accepted Manuscripts* in the [Information for Authors](#).

Please note that technical editing may introduce minor changes to the text and/or graphics, which may alter content. The journal's standard [Terms & Conditions](#) and the [Ethical guidelines](#) still apply. In no event shall the Royal Society of Chemistry be held responsible for any errors or omissions in this *Accepted Manuscript* or any consequences arising from the use of any information it contains.

Time evolution of foam  
height for different bilayer  
volume fractions  $\Phi$  in  
lamellar phases



## On the stability of foams made with surfactant bilayer phases

Zenaida Briceño<sup>1,2</sup>, Amir Maldonado<sup>3</sup>, Marianne Impérator-Clerc<sup>1</sup>, Dominique Langevin<sup>1\*</sup>

<sup>1</sup>Laboratoire de Physique des Solides, UMR CNRS 8502, Université Paris Sud 11, 91400 Orsay Cedex, France

<sup>2</sup>Departamento de Investigación en Polímeros y Materiales de la Universidad de Sonora Blvd. Luis Encinas y Rosales s/n, 83000, Hermosillo, Sonora, México

<sup>3</sup>Departamento de Física de la Universidad de Sonora Blvd. Luis Encinas y Rosales s/n, 83000, Hermosillo, Sonora, México

\* Corresponding author.

### Abstract

The stability of foams made with sponge phases ( $L_3$  phases) and lamellar phases ( $L_\alpha$  phases), both containing surfactant bilayers, has been investigated. The extreme stability of foams made with lamellar phases seems essentially due to the high viscosity of the foaming solution, which slows down gravity drainage. Moreover, the foams start draining only when the buoyancy stress overcomes the yield stress of the  $L_\alpha$  phase. The bubble growth associated to gas transfer is unusual: it follows a power law with an exponent smaller than those corresponding to Ostwald ripening (wet foams) and to coarsening (dry foams). The foams made with sponge phases are in turn very unstable, even less stable than pure surfactant foams made with glycerol solutions having the same viscosity. The fact that the surfactant bilayers in the sponge phase have a negative Gaussian curvature could facilitate bubble coalescence.

## 1. Introduction

Liquid foams are dispersions of gas in liquid, stabilized by surface active agents such as surfactants, polymers or particles (1). Because of gravity, the liquid drains out rapidly and the resulting structure is composed of polyhedral gas bubbles, separated by thin liquid films, themselves connected to a network of liquid channels called *Plateau borders*. Foams have numerous applications in detergency, food products, cosmetics, fire-fighting, oil recovery, among others.

It was noted early by Friberg that when the liquid used is a surfactant *lamellar phase*, the foams were extremely stable (2). He found that even foams made with non-aqueous solvents, notoriously unstable in general, can become stable if lamellar phases are present (3). Lamellar phases are liquid crystalline phases frequently formed in concentrated surfactant solutions: they are made of ordered stacks of surfactant bilayers separated by water. They are optically anisotropic and their presence can be revealed by placing them between crossed polarizers (4). Friberg and collaborators identified in this way the presence of a lamellar organization in the interstices between bubbles (Plateau borders) with foams made with  $L_{\alpha}$  phases (3). In their studies, dispersions of lamellar phases in the solvent (water, hydrocarbons or their mixtures) were used, i.e. two-phase systems containing aggregates such as multilamellar vesicles. The foam stabilization was attributed to the prevention of liquid drainage and to the enhancement in mechanical strength of the liquid films between bubbles (5, 6). Very similar observations were made with emulsions, which can be also efficiently stabilized if lamellar phases are used, and for similar reasons (5). This is particularly important in food products where lamellar structures are frequently present (7).

Garrett and Gratton showed later that the vesicles exhibit rates of transport to air-water surfaces lower than individual surfactant molecules, which leads to lower foamabilities. However the stability of the resulting foams was generally enhanced (8). Recent experiments were performed below the surfactant Krafft temperature at which the surfactant chain crystallise and the bilayers become solid. The corresponding lamellar phases are called  $L_{\beta}$  phases. As postulated by Friberg, the foams were shown to be stabilized not only by strong interfacial films but also by agglomerated self-assemblies within the Plateau borders (9). Curschellas and coworkers showed that the adsorption of the multilamellar vesicles present in the bulk solutions leads to a multilayered film at the air-water interface (10). Shrestha and coworkers (11, 12), Yan and coworkers (13) and Li and coworkers (14) showed that in other systems, the particles remained intact at the air-water surface and that the foams were stabilized by the dispersed solid particles.

Dispersions made with pure lamellar phases have been comparatively less studied, only a few studies of emulsions made with thermotropic liquid crystals were reported (15). The aim of these studies was to find ways of controlling the spatial organizations of emulsion drops and the anisotropic interactions between them. The literature on foams made with pure lamellar phases is still scarcer (16).

In the present study, we have used ternary mixtures of salted water (brine), surfactant and alcohol. Lamellar phases, called  $L_{\alpha}$  phases are formed for certain surfactant/alcohol ratios, in which the surfactant chains are liquid-like (at the difference of the  $L_{\beta}$  phases). It is possible to vary the rheological properties of these lamellar phases by changing the surfactant + alcohol content.

Furthermore, no particles are present. The stabilization mechanisms of the foams are therefore expected to be different than those proposed in references (11-13). When the relative amount alcohol/surfactant is increased, a different phase called  $L_3$  phase is obtained, also made of bilayers, but without long range order. Its structure is bicontinuous, with two intertwined networks of water and bilayers, the bilayers being interconnected through *passages*. This is why this phase is also called *sponge phase* (4). Our study is based on a previous very complete rheological investigation of the foaming liquids (17) and includes foam drainage and coarsening measurements. A comparison of the foam stability between the two different bilayer phases ( $L_\alpha$  and  $L_3$ ) was also performed.

## 2. Material and methods

The foaming solutions are made with purified water (Millipore) to which 20g/L sodium chloride is added. The surfactant used is Sodium Dodecyl Sulfate (SDS) and the alcohol is hexanol. The chemicals were purchased from Sigma and used as received. The phase diagram of the system is shown in figure 1.

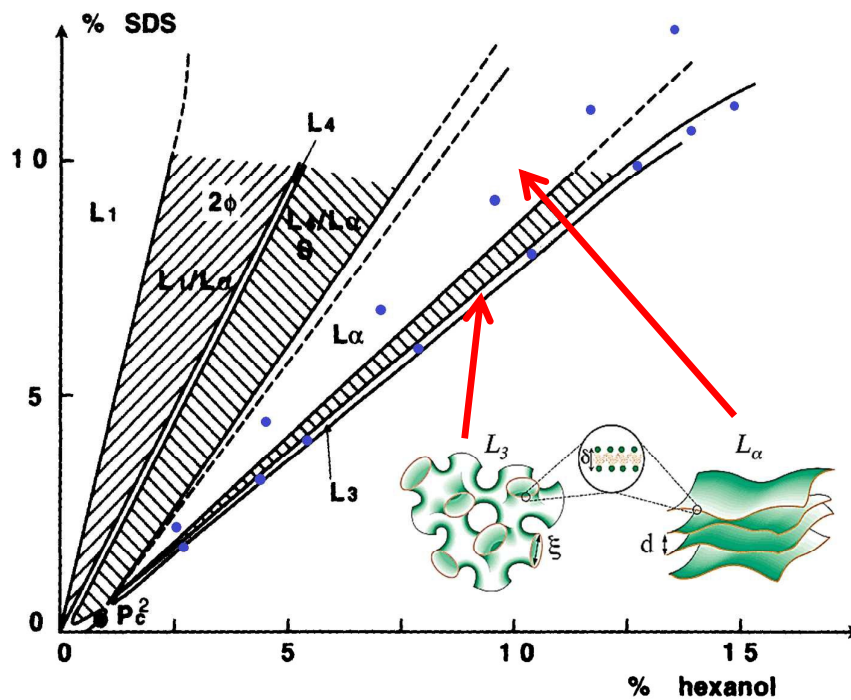


Figure 1. Partial phase diagram of the SDS-hexanol-brine (NaCl 20 g/L) system, adapted from (18, 19). The points in the lamellar phase  $L_\alpha$  and sponge phase  $L_3$  correspond to the samples used in the present study. Percentages are mass %. Temperature is 25°C.  $L_1$  is an isotropic phase containing surfactant micelles.  $L_\alpha$  is a lamellar phase.  $L_3$  and  $L_4$  are, respectively, a sponge phase and a vesicle phase. The region S is a two-phase region where phases  $L_4$  and  $L_\alpha$  coexist.

Figure 1 shows that  $L_{\alpha}$  and  $L_3$  phases can be found in this system. The phase limits are straight lines going through the water corner. This means that phases with increasing amount of bilayer but constant ratios of surfactant to alcohol can be studied. We will call  $\Phi$  the volume fraction of the bilayers, i.e. the sum of the volume fractions of alcohol and surfactant in these phases.

The rheological characterization of the  $L_{\alpha}$  and  $L_3$  phases was performed and is described elsewhere (17). The  $L_3$  phases are purely viscous and Newtonian at the measured shear rates ( $0.01$ - $1000 \text{ s}^{-1}$ ). Their viscosities  $\eta$  are given in Table 1. The  $L_{\alpha}$  phases are viscoelastic, with a shear storage modulus  $G'$  about ten times larger than the loss modulus  $G''$ . The yield stress  $\sigma_Y$  of these  $L_{\alpha}$  phases is however rather low. The values of  $G'$  at low strain, of the yield stress  $\sigma_Y$  and of the viscosity  $\eta$  at the onset of flow are given in Table 1 for the different bilayer volume fractions  $\Phi$  in the  $L_3$  and  $L_{\alpha}$  phases. The viscosities  $\eta$  were estimated using  $\eta = \sigma_Y/\dot{\gamma}$ .

Bilayer volume fraction $\Phi$	$L_3$ phase	$\eta$ (mPa.s)	$L_{\alpha}$ phase	$G'$ (Pa)	$\sigma_Y$ (Pa)	$\eta$ (Pa.s)
				strain<1% frequency $10\text{s}^{-1}$	initial shear rate $0.01\text{s}^{-1}$	
0.05		3.42		1.83	0.032	3.2
0.08		4.13				
0.10		4.36		3.58	0.107	10.7
0.15		5.21		7.73	0.262	26.2
0.20		6.22		16.4	0.319	31.9
0.25		7.25		22.7	0.404	40.4
0.28		8.12				
0.30		8.37		42.7	0.653	65.3

Table 1. Rheological parameters of the  $L_3$  and  $L_{\alpha}$  phases studied.  $L_3$  phases: viscosity  $\eta$ ;  $L_{\alpha}$  phases: shear storage modulus  $G'$  at low strain, yield stress  $\sigma_Y$  and viscosity  $\eta$  at the onset of flow. Data from (17)

Above the yield stress, the lamellar phases flow showing appreciable shear thinning, typically a viscosity decrease by a factor of 10 when the shear rate  $\dot{\gamma}$  varies between  $0.01$  and  $10 \text{ s}^{-1}$ . When the shear rate reaches a critical value close to  $10 \text{ s}^{-1}$ , the viscosity increases, exhibits a maximum and decreases again. This maximum was attributed to the formation of multilamellar vesicles (*onions*) (17). If the shear is lowered to values smaller than the critical shear rate, the onions disappear after typically 15 minutes, and extended lamellae reform. Note that in ref (20), some foams were reported to be stabilized by  $L_{\alpha}$  particles, likely onions as well, but their lifetime was probably much longer than those formed by our solutions.

The foams were produced using a device made of two identical plastic syringes connected by a narrow tube. One syringe is first filled with a controlled amount of gas and liquid, the total volume being  $60 \text{ cm}^3$  (total length of about  $10 \text{ cm}$ ). A series of compression/expansion cycles (10 in total) is then performed, in which the content of one syringe is emptied in the second one, the pistons of the two syringes being controlled by a motor. This device produces foams of well-defined initial gas fraction  $\varepsilon_0$  and very small bubble diameters (a few tens of microns) (21).

In the present study, the initial volume of the gas is 40 mL for a total volume of 60 mL. When all the gas is incorporated in the foam, the initial gas fraction in this foam is 0.66. It was in fact impossible to incorporate the 40 mL of gas in foams of lamellar phases with  $\Phi > 0.10$ , because the very high viscosity values of the lamellar phases renders the mixing procedure less effective. Hence the initial gas fraction  $\varepsilon_0$  in these foams is smaller than the expected 0.66. At the end of the foaming process, the foams produced are transferred to glass burettes in order to study drainage and subsequent foam evolution. In the case of the sponge phase, the foam evolution is much more rapid. The study was also made directly in the production syringes which were removed from the piston device and set vertically. The evolutions observed in the plastic syringe and in the glass burette are identical.

The smallest surfactant concentration used corresponds to  $\Phi = 5\%$ , i.e. about 23 g/L. This is much larger than the minimum amount needed,  $C_{ads}$ , in order to cover the bubbles surfaces in the foam generated. Indeed:  $C_{ads} \sim 6 \varepsilon M_s / [\mathcal{N} \Sigma D (1-\varepsilon)]$ ,  $M_s$  being the surfactant molecular weight,  $\mathcal{N}$  the Avogadro number,  $\Sigma$  the area per surfactant molecule at the bubble surface,  $\varepsilon$  the gas fraction and  $D$  the bubble diameter. For the bubbles produced with the solution  $\Phi = 5\%$ , the initial bubble diameter is 50  $\mu\text{m}$  (figure 3). Using  $\varepsilon = 0.66$ ,  $M_s = 288$  g and  $\Sigma \sim 0.5$  nm<sup>2</sup>/molecule, one finds  $C_{ads} \sim 0.2$  g/L, i.e. much smaller than the total surfactant concentration. We conclude that despite the domains of existence of the  $L_\alpha$  and  $L_3$  phases are narrow, the loss of surfactant used to coat the bubbles is much too small to affect the structure of the phases used. As a matter of fact, no phase separation was ever observed in the liquid of the foam.

The time evolution of bubble size was also determined. For this purpose, small foam samples (1-2 mm thick) are extracted at the top of the syringe, set vertically as for height measurements. The first sample is discarded and the second is carefully spread at the surface of a glass slide, in order to form a monolayer of bubbles. This layer is then covered by a second slide and immediately transferred to a microscope stage. Images of the bubbles are then taken and the bubble size distribution is obtained by using the Image J software.

### 3. Results. Foams made with lamellar phases

Figure 2 shows pictures of the bubbles, figure 2A being taken without polarizers, figures 2B and C between cross polarizers.

Figures 2B and C evidence the presence of a liquid crystalline organization between the bubbles, likely lamellar, because of the typical birefringent texture. At the difference of earlier studies (12, 13, 20, 22, 23), no particles are observed at the surface of the bubbles. The brightness of the pictures between crossed polarizers increases with time during days, suggesting a slow reorientation of the lamellae with respect to the glass slides (figure 2C).

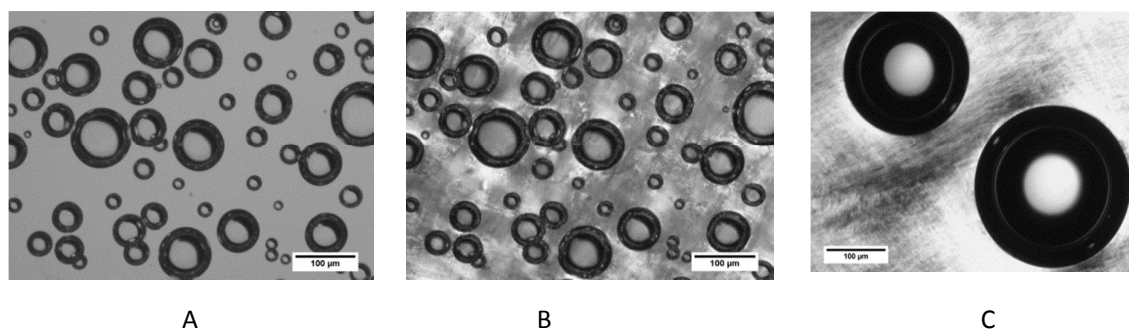


Figure 2. Optical microscopy pictures of bubbles in the foam made from the lamellar phase with  $\Phi = 0.30$ . Pictures A&B were taken 10 minutes after foam production: A without crossed polarizers and B with crossed polarizers. Picture C was taken 8 days after foam production, between crossed polarizers

The bubbles always appear spherical. They are sometimes deformed during the preparation, but relax rapidly to a spherical shape. This is because the stress due to capillary pressure  $4\gamma/D$  is always much larger than the yield stress  $\sigma_y$  ( $4\gamma/D \sim 3000$  Pa, with  $\gamma = 35$  mN/m (value at the critical aggregation concentration, see appendix,  $D \sim 50\mu\text{m}$ , while  $\sigma_y < 1$  Pa, see table 1 ). The relaxation time  $\tau$  is very short, of order  $\eta D/\gamma$  which is between 0.01 and 0.1s, according to the viscosities quoted in table 1.

The initial bubble size distribution in the foams made with lamellar phases is shown in figure 3.

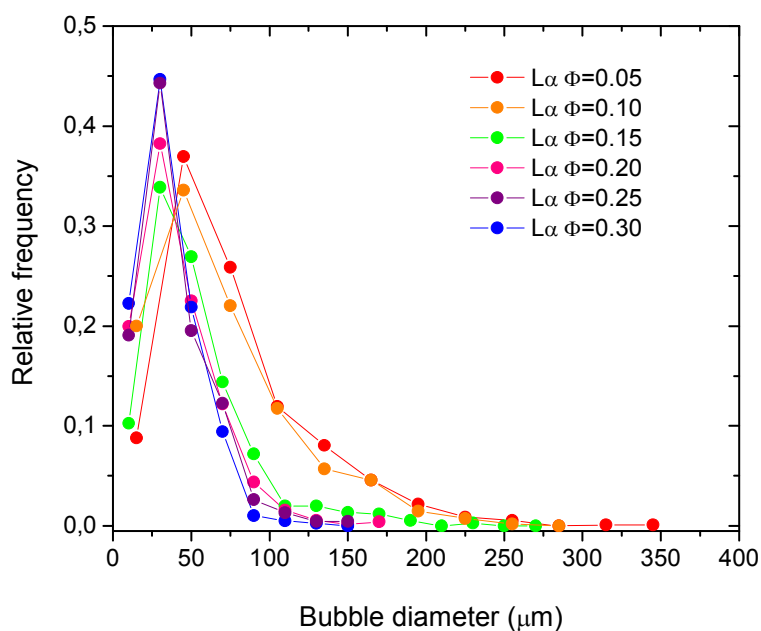


Figure 3. Initial size distribution of the bubbles in the foams made with the lamellar phases. The different colors correspond to different bilayer volume fractions  $\Phi$  in the foaming liquid.

Figure 3 shows that very small bubbles are produced with the foaming device used, the mean size decreasing as the viscosity increases as currently observed with the device used (21). Figure 4 shows a set of pictures illustrating the time evolution of the samples:

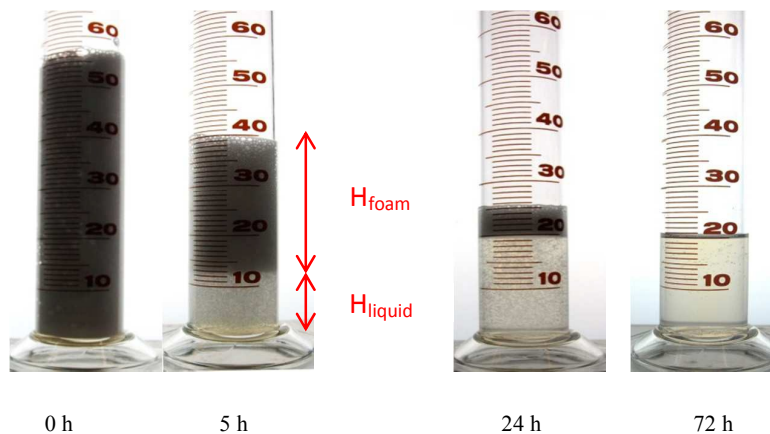


Figure 4. Time evolution of foams made with the lamellar phase with  $\Phi = 0.10$ .

The stability of the foams made with lamellar phases is extremely good. Figure 5 shows the time evolution of the foam height and of the liquid or solid fraction in the foam. Due to the fact that the lamellar phase has a non-zero shear modulus and does not flow in the limit of small deformations, the continuous phase of the foam is solid in this case.

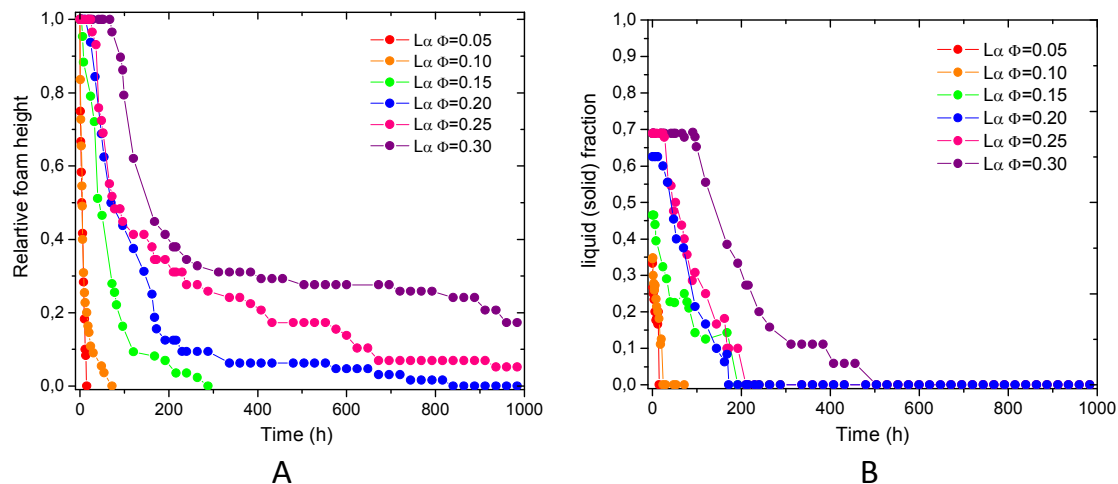


Figure 5. Time evolution of : A : Relative foam height (with respect to the height at time zero). B : liquid fraction in the foam (solid fraction, when the lamellar phase does not flow). The different colors correspond to different volume fractions  $\Phi$  of bilayers in the foaming liquid.

The foam containing the smallest concentration of bilayers ( $\Phi = 0.05$ ) collapses rapidly, but when  $\Phi$  increases, the foam lifetime becomes extremely long (a month for  $\Phi = 0.20$  and still longer above). Figure 5B shows that the initial liquid (solid) fraction in the foams with  $\Phi > 0.10$  is larger than the expected 0.33, since  $\varepsilon_0 < 0.66$ , as already mentioned in § 2.

## 4. Discussion

### 4.1 Onset of drainage and foam coarsening

After a lagtime that depend on  $\Phi$ , the foams drain until very low liquid fractions are reached. This is somewhat unexpected because  $L_\alpha$  phases are solid like, with a  $G'$  larger than  $G''$ . However, the yield stresses are low and drainage could proceed once the internal stress  $\sigma$  exceeds the yield stress. We can estimate  $\sigma$  by calculating the buoyancy force per unit area exerted between the bubble and the lamellar phase :  $\sigma = \rho g D/6$ ,  $\rho$  being the lamellar phase density,  $g$  the gravity constant and  $D$  the mean bubble diameter. With  $\rho \sim 1000 \text{ Kg/m}^3$ ,  $g \sim 10 \text{ m/s}^2$  and  $D \sim 50 \mu\text{m}$ , one finds  $\sigma \sim 0.08 \text{ Pa}$ , larger than the yield stress for the lamellar phases with  $\Phi = 0.05$ . The corresponding foam is therefore expected to drain, as observed. The foams made with the lamellar phases of higher  $\Phi$  do not drain at short times since  $\sigma_y > \sigma$ , but drainage starts later. This is likely due to the increase of the bubble diameter with time: if  $D$  increases, so does the buoyancy force. This increase originates from pressure differences between bubbles: Ostwald ripening for wet foams ( $\varepsilon < 0.64$ ) and coarsening for drier foams ( $\varepsilon > 0.64$ )(1). Similar observations of delayed drainage were reported for foams made from other viscoelastic fluids possessing a yield stress : clay dispersions (24), emulsions (25, 26), vesicles (9) and particles (27).

We have measured the time evolution of the bubble diameter for the samples with  $\Phi = 0.10$  and 0.30. Figure 6 shows the results. The bubble diameter scales as  $t^\beta$  with  $\beta \sim 0.25$ , lower than expected for coarsening ( $\beta = 0.5$ ) and even for Ostwald ripening ( $\beta = 0.33$ ) (1).

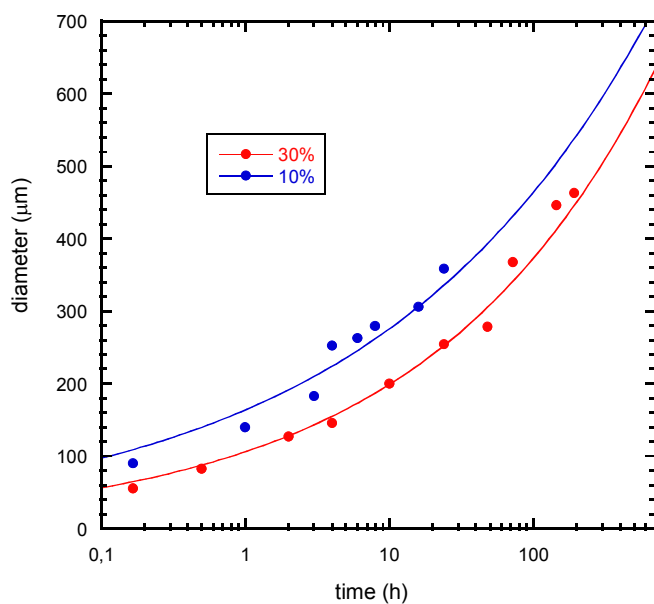


Figure 6. Time evolution of the bubble diameter for the samples made with  $\Phi = 0.10$  and 0.30. The line are fits to power laws  $D \sim t^\alpha$ , with  $\alpha = 0.23$  for  $\Phi = 0.10$  and  $\alpha = 0.27$  for  $\Phi = 0.30$ .

Such a small exponent  $\beta$  was found previously in foams made with pure nematic and smectic liquid crystals ( $\beta = 0.2$ ) and was attributed to the local stresses due to orientation defects (28). The fact that the exponents  $\beta$  measured in our study are smaller than the classical  $\beta$  exponents could be due to similar effects. Note that no anomaly was found for the exponent measured with 2D foams made with pure liquid crystals (16).

The foams made with  $\Phi = 0.10$  start draining very quickly. Indeed, the critical diameter  $D^* = 6\sigma_v/\rho g = 60 \mu\text{m}$  is reached early, in 10 sec or so. The foams made with  $\Phi = 0.30$  start to drain only after 200 hours, when the diameter has reached values of  $400 \mu\text{m}$  (figure 6), for which  $\sigma = 0.67 \text{ Pa}$ . This value is in very good agreement with the condition  $\sigma^* = \sigma_v$ , the yield stress being  $0.65 \text{ Pa}$  for  $\Phi=0.30$ .

## 4.2 Foam drainage

The foams obtained for large  $\Phi$  are initially dispersions of bubbles (bubbly liquids, initial gas fraction  $\varepsilon_0 < 0.64$ ), because all the gas could not be incorporated. In this case, the bubbles rise at a velocity  $V$  that we will estimate using the Stokes' expression:

$$V = \frac{1}{18} \frac{\rho g D^2}{\eta} \quad (1)$$

In this expression, the hydrodynamic interactions between neighboring bubbles have been neglected.

One could roughly estimate the velocity of drainage using the time evolution of the liquid fraction (figure 5). The times  $\tau_{\text{drain}}$  required to drain half the liquid is about 50 hours for the more concentrated samples (after drainage starts). This time corresponds to a velocity of about  $10^{-7} \text{ m/s}$ , and to a local velocity gradient  $\dot{\gamma}$  of order  $10^{-3} \text{ s}^{-1}$  assuming a characteristic distance between bubbles of the order of the bubble diameter, i.e. about  $200 \mu\text{m}$  after a few hours (figure 6). At these low shear rates, the viscosities of the concentrated samples are very high, of order of tens of  $\text{Pa}\cdot\text{s}$  (table 1). Equation 1 leads to a velocity of bubble rise of about  $10^{-7} \text{ m/s}$ , consistent with the observations, in view of the crude assumptions made.

The estimations are more difficult to make for the smaller  $\Phi$ , because equation 1 no longer holds. When the gas fraction is sufficiently large ( $\varepsilon > 90\%$ ), the factor  $1/18$  in equation 1 has to be replaced by  $K(1-\varepsilon)^\alpha$ ,  $K$  being a permeability coefficient ( $K \sim 10^{-3}$ ) and the exponent  $\alpha$  being equal to 1 for rigid interfaces and to  $1/2$  for mobile ones (1), such as in pure SDS foams (29). Since no expression for the drainage velocity is available in the intermediate gas fraction range, we have not tried to analyze the corresponding drainage times.

## 4.3 Foam lifetime

Figure 7 shows the time evolution of the drained liquid height (empty circles) and of the total height foam+ liquid (filled circles). The total height decreases since the beginning for the foams with small  $\Phi$  (5 and 10%). This decrease demonstrates that the foam height decrease shown on figure 5A is not only due to drainage (and loss of liquid in the foam), but that the gas volume decreases also. Such a decrease could be due to coarsening of the bubbles adjacent to the interface, but coarsening is slow and the corresponding volume of lost gas very small. The gas volume decrease is more likely due to bubble destruction at the top of the foam, destruction events being indeed observed by visual

inspection. At the end of drainage, the foams with small  $\Phi$  have fully collapsed, a typical behavior of very unstable foams. The long lifetimes observed are a mere consequence of the large viscosity that slows down considerably foam drainage (at shear rates of  $0.01 \text{ s}^{-1}$ , the liquid viscosity is of order  $10 \text{ Pa}\cdot\text{s}$ , i.e.  $10^4$  times larger than the viscosity of pure water).

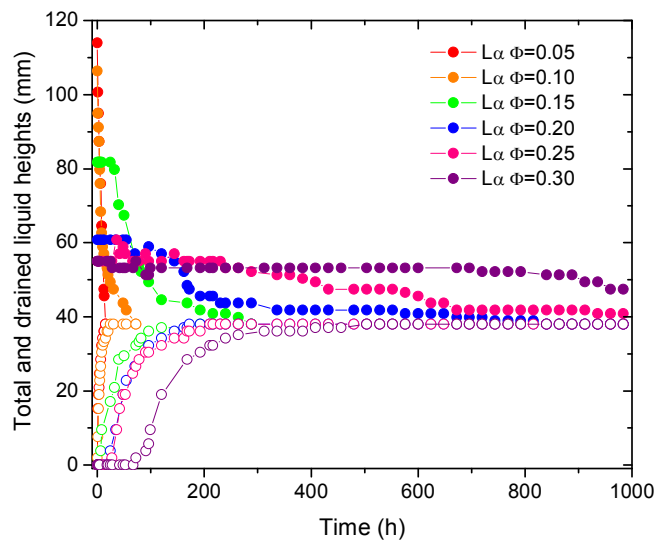


Figure 7. Height of drained liquid (empty symbols) and total height of foam + drained liquid (closed symbols) versus time for the different lamellar phases.

The foams made with the more concentrated samples ( $\Phi = 0.15$  to  $0.30$ ) survive an appreciable time especially those for  $\Phi = 0.25$  and  $0.30$ . The foams with  $\Phi = 0.30$  start collapsing only after  $700 \text{ h}$ , when the bubble diameter is  $600 \mu\text{m}$  (as seen in figure 6). The foam height at the beginning of collapse is  $15 \text{ cm}$  (figure 7) and according to (30), it corresponds to an equilibrium liquid fraction of  $0.05$  at the top of the foam. From these numbers, one can estimate the capillary pressure  $P_{\text{cap}}$  at the top of the foam and at the onset of collapse. By using:  $P_{\text{cap}} = 2\gamma/(D\sqrt{\phi})$  (1), one finds  $P_{\text{cap}} \sim 500 \text{ Pa}$ . It has been shown that foams collapse once  $P_{\text{cap}}$  reaches a critical pressure  $P_{\text{cap}}^*$  at which the foam films rupture (31-34). Unfortunately, the high viscosity of the liquids used prevented us to study the foam films in a thin film balance and to directly measure  $P_{\text{cap}}^*$  as in the previous studies. In the case of films made with SDS and large salt concentrations ( $0.1\text{M}$ ) as here, it was reported that the foam films are Newton black films, i.e. surfactant bilayers containing very small amounts of water (hydration water), and that  $P_{\text{cap}}^* \sim 70 \text{ kPa}$  (35). In the present case, the bubble surfaces are covered by mixed SDS-hexanol monolayers, which could be more compressible than pure SDS monolayers, hence more susceptible to thermal fluctuations in surface coverage. As a consequence, the critical pressure  $P_{\text{cap}}^*$  could be smaller (32). However, surface tension measurements suggest that they are rather rigid (see appendix), hence  $P_{\text{cap}}^*$  could be very large instead. It is however known that  $P_{\text{cap}}^*$  decreases when the film size increases. Unfortunately, this variation has been little studied to date, so it is difficult to conclude about the exact role of  $P_{\text{cap}}^*$  in the foams studied.

## 5. Foams made with sponge phases

Although the amount of hexanol is not much higher in the sponge phases than in the lamellar phases (figure 1), the sponge phases are Newtonian fluids with small viscosities (Table 1). The stability of foams made with these liquids is very limited. Figure 8 shows the time evolution of the drained liquid height and of the total foam+drained liquid height.

The foams made with the smallest  $\Phi$  (0.05-0.10) start collapsing as soon as drainage starts. The foams made using the more concentrated sponge phases ( $\Phi = 0.15-0.30$ ) are somewhat more stable and initially coarsen (the gas volume remaining constant) before collapsing.

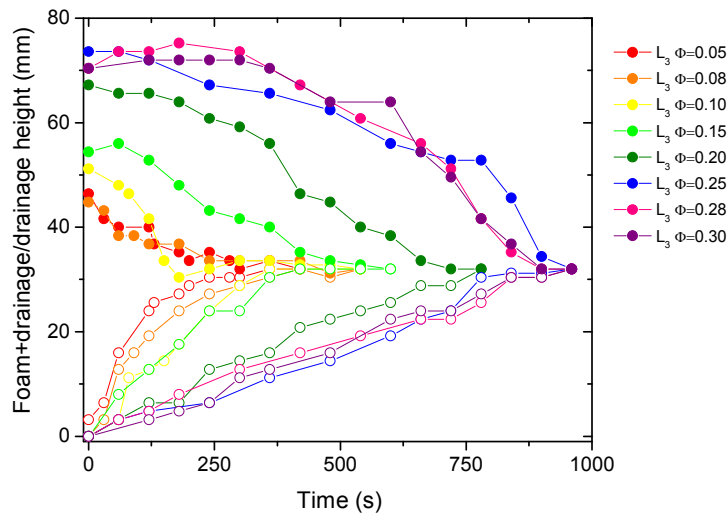


Figure 8. Height of drained liquid (empty symbols) and total height of foam + drained liquid (closed symbols) versus time for the different sponge phases.

Figure 9 shows the half lifetime  $\tau$  of the foam (defined as the time after which the initial foam height has decreased by a factor 2) as a function of the viscosity. This time is about ten times smaller than that for pure SDS foams made from mixed water-glycerol solutions, with similar bulk viscosities (36). While  $\tau$  varies linearly with viscosity for the SDS foams, in the case of the sponge phase, there is a change in behavior between the more dilute and the more concentrated sponge phases. This change likely reflects the changes observed in figure 8: rapid collapse of foams at low  $\Phi$  and collapse preceded by a coarsening step at high  $\Phi$ .

One could wonder why phases containing similar amounts of hexanol could have rheological properties that are so different. It was also observed that the viscosity of the sponge phase does not extrapolate to the viscosity of water  $\eta_w$  upon dilution (see figure 9). It was postulated by Snabre and Porte that this behavior originates from the fact that applied stresses are relaxed through viscous drags of both surfactant in the bilayers (viscosity  $\eta_s$ ) and of water in the network of passages (viscosity  $\eta_w$ ), without breaking of the passages (37). The model leads to a viscosity variation of the type  $A\eta_w(1-\Phi) + B\eta_s\Phi$ , in agreement with the measurements. Lamellar phases are stacks of bilayers separated by water layers, without water passages: water transport implies essentially permeation

across the bilayers, a very long process. Furthermore,  $L_\alpha$  phases have uniaxial symmetry, they are solid like and have a non-zero shear moduli. The measured moduli are small, because the phases are not monocrystalline and contain orientation defects, but despite of this, they behave as solids. The yield stress is also small, but large enough to result in high viscosities at low shear rates  $\dot{\gamma}$ .

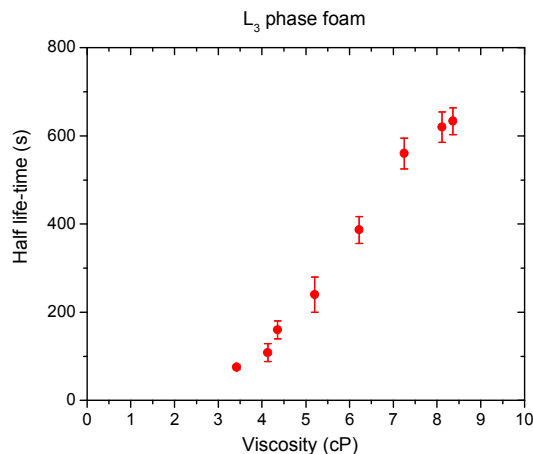


Figure 9. Half lifetime  $\tau$  of foams made from the sponge phases versus the viscosity of the liquid phases. The points correspond to  $\Phi$  values increasing between 0.05 and 0.3, increasing from left to right.

The surface tension of sponge phases and of lamellar phases is the same for a given  $\Phi$  in our study (see Appendix). This suggests that the surfactant surface concentrations are the same and that the surface elastic properties should be similar. It has been shown in similar systems that the bending constants for mean curvature of the surfactant monolayers were also the same in the  $L_\alpha$  and in the  $L_3$  phase (38). The difference in structure is related to the bending constant for Gaussian curvature that changes appreciably upon addition of alcohol, because of bilayer curvature frustration (38).

The bilayers are frustrated in the  $L_3$  phase, passages form easily and could facilitate coalescence of bubbles. Indeed, due to the high concentration of added salt, the foam films are very thin and are made of bilayers. If holes are easily formed in these bilayers, coalescence will become easy.

One could therefore expect that film rupture occurs easily after foam film drainage. We have calculated the film drainage time using the Reynolds formula that applies for films reaching very small thicknesses such as the NBF in the present foams (39) :

$$V_{film} = \frac{h^3 P_{cap}}{3 \eta r^2}$$

where  $h$  is the film thickness and  $r$  the film radius, of order  $D/3$ . The film drainage time is therefore:

$$t_{film\ drainage} = \frac{6 \eta r^2}{h^2 P_{cap}}$$

Using a viscosity  $\eta = 3 \text{ mPa}\cdot\text{s}$  (foam with  $\Phi = 0.05$ ),  $r=30\mu\text{m}$  ( $D=100\mu\text{m}$ ),  $P_{\text{cap}} = 5000 \text{ Pa}$  (corresponding to a liquid fraction of 2% after drainage (30)) and an equilibrium thickness  $h = 5 \text{ nm}$ , one estimates a film drainage time of 100 s, comparable to the foam lifetimes as expected.

## 6. Conclusion

The stability of the foams made with sponge phases ( $L_3$ ) and lamellar phases ( $L_\alpha$ ) are very different. The extreme stability of the foams made with lamellar phases seems essentially due to the high viscosity of the foaming solution. Note that this stabilization mechanism is completely different to that observed in foams made with other type of bilayers phases ( $L_\beta$ ), stabilized by adsorption of  $L_\beta$  particles at the surface of the bubbles.

Despite  $L_\alpha$  phases having finite yield stresses, the buoyancy stress exerted by bubbles is able to overcome this yield stress and the foams drain. If the bubbles are too small, a lag time is necessary to allow sufficient bubble growth through coarsening (or Ostwald ripening). The foams made with the most viscous  $L_\alpha$  phases appear to last for some time after drainage has stopped, but the capillary pressures in the foams seem too low to account for film rupture.

The bubble growth associated to gas transfer is unusual, and follows a power law with an exponent smaller than that corresponding to Ostwald ripening (wet foams) or coarsening (dry foams). The reason for this is not yet clear.

The foams stabilized by sponge phases are very unstable, much less stable than pure surfactant foams made with solutions having the same viscosity. The fact that the bilayers are frustrated and easily form passages could facilitate coalescence of bubbles.

## 7. Acknowledgements

We are grateful to Delphine Hannoy for performing the surface tension measurements and to Anniina Salonen for a critical reading of the manuscript. We acknowledge fruitful discussions on the rheology of lamellar and sponge phases with Pawel Pieranski. Z.B acknowledges financial support from Conacyt and European Space Agency.

## Appendix

The surface tension of aqueous solutions containing salt (20g/L sodium chloride) and various amounts of SDS and hexanol, keeping the ratio SDS/hexanol constant (1 for lamellar phases and 0.75 for sponge phases) has been measured as a function of SDS concentration. We used a Tracker instrument from Teclis with an automatic dilution procedure. The results are shown in figure A1

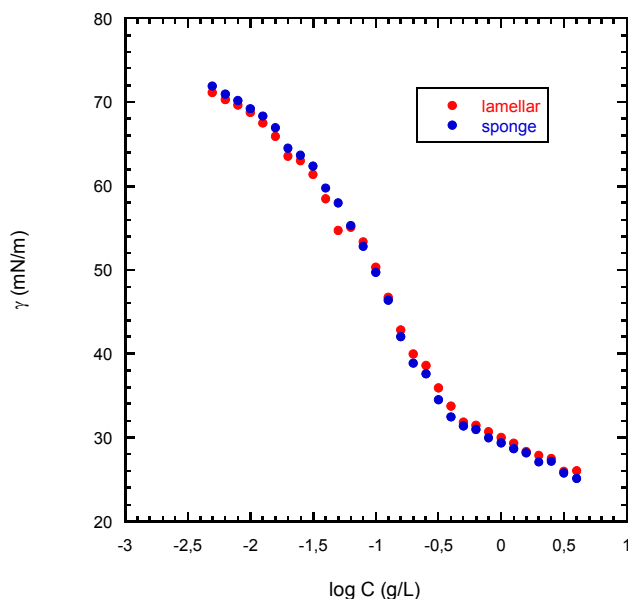


Figure A1. Surface tension for brine solutions versus SDS concentration. The mass ratio of SDS/hexanol is 1 for the lamellar phase (red dots) and 0.75 for the sponge phase (blue dots).

For a given bulk surfactant concentration  $C$ , the surface tensions of the two types of solutions are the same within error bars. There is a break point around 0.3 g/L. This value is comparable to the critical micellar concentration 0.4g/L for pure SDS in the presence of 0.1M NaCl (values for the salt concentration used here are not available in the literature). Because when concentrated, these solutions are bilayer phases, the break point cannot be a critical micellar concentration, but rather a critical aggregation concentration (CAC) above which bilayers form. This is supported by the fact that the solutions with SDS/hexanol=1 become turbid, suggesting the formation of vesicles.

We calculated the surface concentration  $\Gamma$  using the Gibbs equation below the CAC :

$$\Gamma = -\frac{1}{k_B T} \frac{d\gamma}{d \ln C} \quad (\text{A1})$$

where  $k_B$  is the Boltzmann constant and  $T$  the absolute temperature,. This equation is valid in the presence of excess salt ( $C_{\text{salt}} \gg C$ ). However the surface concentration calculated in this way will be correct only if the SDS and hexanol can be treated as a single species, i.e. if the SDS/hexanol ratio is the same in the bulk solution and at the surface. This could not be the case, but equation A1 will at least give us an order of magnitude. By fitting the surface tension curve by a polynomial and performing a numerical derivation, we find that close to the CAC:  $\Gamma \sim 7.5 \cdot 10^{11}$  molecules/m<sup>2</sup> and  $1/\Gamma$

$\sim 17\text{\AA}^2$  per molecule. This value is very small ( $1/\Gamma \sim 50\text{\AA}^2$  for pure SDS) but it corresponds in fact to the group of molecules SDS-hexanol.

We have also calculated the intrinsic surface compression modulus using :

$$E = -\Gamma \frac{\partial \gamma}{\partial \Gamma} \quad (\text{A2})$$

and found quite large values,  $E \sim 100\text{mN/m}$ . We did not attempt to directly measure  $E$  with the Tracker instrument using sinusoidal surface area variations. Indeed, the CAC is too high and at the frequencies available with the instrument, the compression of the surface layer is short-circuited by surfactant diffusion in the bulk, and the mean effective modulus is zero.

## References

1. Cantat I, Cohen-Addad S, Elias F, Graner F, Hohlner R, Pitois O, et al. *Foams - Structure and Dynamics*: Oxford University Press; 2013. 265 p.
2. Friberg S, Ahmad SI. Liquid crystals and foaming capacity of an amine dissolved in water and para xylene. *Journal of Colloid and Interface Science*. 1971;35(1):175-8.
3. Friberg SE, Chang Sup W, Greene B, Van Gilder R. A nonaqueous foam with excellent stability. *Journal of Colloid and Interface Science*. 1984;101(2):593-5.
4. Evans F, Wennerström W. *The Colloidal Domain*. second ed: Wiley; 1999.
5. Friberg SE, Solans C. The Kendall award address - surfactant association structures and the stability of emulsions and foams. *Langmuir*. 1986;2(2):121-6.
6. Friberg SE. Amphiphilic association structures and thin films. *Langmuir*. 1992;8(8):1889-92.
7. Friberg S, Larsson K, Sjoblom J. *Food Emulsions*: CRC Press; 2003.
8. Garrett PR, Gratton PL. Dynamic surface tensions, foam and the transition from micellar solution to lamellar phase dispersion. *Colloids and Surfaces a-Physicochemical and Engineering Aspects*. 1995;103(1-2):127-45.
9. Varade D, Carriere D, Arriaga LR, Fameau AL, Rio E, Langevin D, et al. On the origin of the stability of foams made from cationic surfactant mixtures. *Soft Matter*. 2011;7(14):6557-70.
10. Curschellas C, Kohlbrecher J, Geue T, Fischer P, Schmitt B, Rouvet M, et al. Foams Stabilized by Multilamellar Polyglycerol Ester Self-Assemblies. *Langmuir*. 2013;29(1):38-49.
11. Shrestha LK, Aramaki K, Kato H, Takase Y, Kunieda H. Foaming properties of monoglycerol fatty acid esters in nonpolar oil systems. *Langmuir*. 2006;22(20):8337-45.
12. Shrestha LK, Saito E, Shrestha RG, Kato H, Takase Y, Aramaki K. Foam stabilized by dispersed surfactant solid and lamellar liquid crystal in aqueous systems of diglycerol fatty acid esters. *Colloids and Surfaces a-Physicochemical and Engineering Aspects*. 2007;293(1-3):262-71.
13. Li X-A, Peng J-B, Yan Y-L. Aqueous foam stabilized by polyoxyethylene dodecyl ether. *Chemical Papers*. 2009;63(5):620-4.
14. Zhang L, Mikhailovskaya A, Yazhgur P, Muller F, Cousin F, Langevin D, et al. Precipitating Sodium Dodecyl Sulfate to Create Ultrastable and Stimulable Foams. *Angewandte Chemie-International Edition*. 2015;54(33):9533-6.
15. Poulin P. Novel phases and colloidal assemblies in liquid crystals. *Current Opinion in Colloid & Interface Science*. 1999;4(1):66-71.
16. Trittel T, John T, Stannarius R. Smectic Foams. *Langmuir*. 2010;26(11):7899-904.
17. Briceño Z, Soltero A, Maldonado A, Perez J, Langevin D, Impéror-Clerc M. Effect of shear on the lamellar phase of the SDS-hexanol-brine system. submitted.
18. Auguste F, Bellocq AM, Roux D, Nallet F, Gulik-Krzywicki T. Dilute and concentrated phases of vesicles at thermal equilibrium. Effect of bilayer elasticity. In: Appell J, Porte G, editors. *Trends in Colloid and Interface Science IX*: Steinkopff; 1995. p. 276-9.
19. Porcar L, Hamilton WA, Butler PD, Warr GG. Scaling of structural and rheological response of L-3 sponge phases in the "Sweetened" cetylpyridinium/hexanol/dextrose/brine system. *Langmuir*. 2003;19(26):10779-94.
20. Shrestha LK, Acharya DP, Sharma SC, Aramaki K, Asaoka H, Ihara K, et al. Aqueous foam stabilized by dispersed surfactant solid and lamellar liquid crystalline phase. *Journal of Colloid and Interface Science*. 2006;301(1):274-81.
21. Gaillard T, Roché M, Honorez C, Balan A, Jumeau M, Drenckhan W. Controlled formation of small-bubble foams: a new mechanism in an old technique, in preparation.
22. Chen Z-L, Yan Y-L, Huang X-B. Stabilization of foams solely with polyoxyethylene-type nonionic surfactant. *Colloids and Surfaces a-Physicochemical and Engineering Aspects*. 2008;331(3):239-44.
23. Yan Y-L, Jia X-G, Meng M, Qu C-T. Foam Superstabilization by Lamellar Liquid Crystal Gels. *Chemistry Letters*. 2011;40(3):261-3.

24. Guillermic RM, Salonen A, Emile J, Saint-Jalmes A. Surfactant foams doped with laponite: unusual behaviors induced by aging and confinement. *Soft Matter*. 2009;5(24):4975-82.
25. Goyon J, Bertrand F, Pitois O, Ovarlez G. Shear Induced Drainage in Foamy Yield-Stress Fluids. *Physical Review Letters*. 2010;104(12).
26. Salonen A, Lhermerout R, Rio E, Langevin D, Saint-Jalmes A. Dual gas and oil dispersions in water: production and stability of foamulsion. *Soft Matter*. 2012;8(48):12135-.
27. Lesov I, Tcholakova S, Denkov N. Factors controlling the formation and stability of foams used as precursors of porous materials. *Journal of Colloid and Interface Science*. 2014;426:9-21.
28. Buchanan M. Liquid Crystal Foams: Formation and Coarsening. arXiv:cond-mat/0206477 [cond-matsoft]. 2002.
29. Durand M, Martinoty G, Langevin D. Liquid flow through aqueous foams: From the plateau border-dominated regime to the node-dominated regime. *Physical Review E*. 1999;60(6):R6307.
30. Maestro A, Drenckhan W, Rio E, Hohler R. Liquid dispersions under gravity: volume fraction profile and osmotic pressure. *Soft Matter*. 2013;9(8):2531-40.
31. Exerowa D, Kashchiev D, Platikanov D. Stability and permeability of amphiphile bilayers *Advances in Colloid and Interface Science*. 1992;40:201-56.
32. Bergeron V. Disjoining pressures and film stability of alkyltrimethylammonium bromide foam films. *Langmuir*. 1997;13(13):3474-82.
33. Khristov K, Exerowa D, Minkov G. Critical capillary pressure for destruction of single foam films and foam: effect of foam film size. *Colloids and Surfaces A-Physicochemical and Engineering Aspects*. 2002;210(2-3):159-66.
34. Stubenrauch C, Khristov K. Foams and foam films stabilized by C-n TAB: Influence of the chain length and of impurities. *Journal of Colloid and Interface Science*. 2005;286(2):710-8.
35. Khristov KI, Exerowa DR, Krugljakov PM. Influence of the type of foam films and the type of surfactant on foam stability. *Colloid and Polymer Science*. 1983;261(3):265-70.
36. Briceño Z, Drenckhan W, Langevin D. Coalescence in draining foams made of very small bubbles. in preparation.
37. Snabre P, Porte G. Viscosity of the L3 phase in amphiphilic systems *Europhysics Letters*. 1990;13(7):641-5.
38. Skouri M, Marignan J, Appell J, Porte G. Fluid membranes in the semirigid regime - scale-invariance. *Journal De Physique II*. 1991;1(9):1121-32.
39. Langevin D, Marquez-Beltran C, Delacotte J. Surface force measurements on freely suspended liquid films. *Advances in Colloid and Interface Science*. 2011;168(1-2):124-34.